Eur. Radiol. (2002) 12:549–558
DOI 10.1007/s003300101036

S. Çakırer
M. Başak
A. Mutlu
G. M. Galip

MR imaging in epilepsy that is refractory to medical therapy

Received: 26 January 2001
Revised: 19 April 2001
Accepted: 6 June 2001
Published online: 28 August 2001
© Springer-Verlag 2001

S. Çakırer (✉) · M. Başak · A. Mutlu · G. M. Galip
Department of Radiology,
Neuroradiology Section,
Istanbul Şişli Etfal Hospital,
Istanbul, Turkey
E-mail: scakirer@yahoo.com
Phone: +90-216-4553522
Fax: +90-216-4553522

S. Çakırer
Present address: 67 Ada, Kardelen 4/2,
Daire 37, 81120 Ataşehir, Istanbul, Turkey

Abstract The aim of this study was the assessment of detection rate on MRI and description of MRI findings in patients with medically intractable epilepsy. Seventy-three patients with medically intractable epilepsy between the ages of 0 and 68 years old were evaluated by MRI, on three planes with spin-echo T1, fast spin-echo T2, and fluid-attenuated inversion recovery sequences, and, if necessary, with contrast-enhanced SE T1 sequences. Cerebral infarct regions with atrophy and gliosis in 8 patients, cerebral tumors in 5 patients, hippocampal sclerosis in 16 patients, radial microbrain in 1 patient, cortical dysplasia in 3 patients, pachygyria in 2 patients, subcortical heterotopia in 2 patients, schizencephaly in 3 patients, cerebral hemiatrophy in 2 patients, tuberous sclerosis in 1 patient, herpes encephalitis in 2 patients, Rasmussen's encephalitis in 1 patient, vascular malformations in 5 patients, and no abnormality in 22 patients were detected. Magnetic resonance imaging has a high success rate in detecting structural brain abnormalities, of both temporal and extratemporal locations, associated with medically intractable epilepsy syndromes. So MRI plays a primary role in planning of the treatment, primarily surgical therapy, by detecting structural epileptogenic lesions.

Keywords MR imaging · Epilepsy

Introduction

Epilepsy is a common neurological disorder, affecting 0.5–1 % of the population of the United States [1]. Fifteen to 30 % of these patients have disease that is refractory to medical therapy, and surgery is the most effective method for controlling seizures in this subset of patients [2, 3, 4]. Magnetic resonance imaging plays an important role in locating and defining anatomic epileptogenic foci in the patients with intractable epilepsy. The MRI findings may also indicate the type of treatment or, if the patient is a candidate for surgery/intervention, the type of surgery/intervention. Magnetic resonance imaging is used to identify the surgical approach, the volume of tissue targeted for resection preoperatively, and the relationship between the epileptogenic focus and adjacent functionally important brain areas; thus, MRI may help determine the prognosis of postoperative seizure control for patients [4, 5, 6, 7, 8].

Structural brain abnormalities associated with epilepsy can be detected with a high degree of sensitivity and specificity using MRI. In 1996 Bronen et al. [9] published an article related to a study of 117 epileptic patients, achieving a sensitivity of 95 % and a specificity of 87 % using MRI [10, 11].

Although in the past clinical and electroencephalographic (EEG) findings was used to classify epileptic seizures, MRI has highlighted the utility of using the anatomic substrates that produce the observed electroclinical abnormalities as a basis for classification; hence, MRI can provide critical data to classify and define the epilepsy [12, 13].

In this study we performed MRI imaging of 73 patients with medically intractable epilepsy, described the

Table 1 Magnetic resonance pathologies detected in 73 patients. *DNET* dysembryoplastic neuroepithelial tumor; *AVM* Arteriovenous malformation; *FLAIR* fluid-attenuated inversion recovery

MR pathology	No. and (%) of patients	Imaging characteristics
Cerebral infarct	8 (10.9)	Focal atrophy, infarct, and surrounding gliosis
Herpes encephalitis	2 (2.7)	Uni- or bilateral hemorrhagic infarct areas, especially dominant in medial temporal lobes
Rasmussen encephalitis	1 (1.4)	Frontotemporal location, corticosubcortically located gliosis and atrophy, progressive in time
Intracranial mass lesions	5 (6.8)	Cerebral mass lesions, generally cortical, small in size, well demarcated, mostly in frontotemporal lobes
DNET	1 (1.4)	
Glial tumor	1 (1.4)	
Ganglioglioma	1 (1.4)	
Metastasis	2 (2.7)	
Hippocampal sclerosis	16 (21.9)	Hippocampal cortical hyperintensity in T2-weighted/FLAIR sequences with or without atrophy
Developmental anomalies	14 (19.2)	Radial microbrain: simplified gyral pattern and undermyelination; cortical dysplasia: small abnormal gyri; pachygyria: broad malformed gyri; subcortical heterotopia: dysplastic gray matter band between cortical mantle and ventricular surface; schizencephaly: cleft between cortical mantle and ventricular surface; cerebral hemiatrophy: hemispheric atrophy with calvarial and paranasal sinus hypertrophy; tuberous sclerosis: cortical tubers, subependymal hamartomas
Radial microbrain	1 (1.4)	
Cortical dysplasia	3 (4.1)	
Pachygyria	2 (2.7)	
Subcortical heterotopia	2 (2.7)	
Schizencephaly	3 (4.1)	
Cerebral hemiatrophy	2 (2.7)	
Tuberous sclerosis	1 (1.4)	
Vascular malformations	5 (6.8)	AVM: dilated arteries and veins with a nidus; cavernoma: hemorrhages in various stages and gliotic capsule (popcorn appearance); venous angioma: dilated veins draining into a large central vein (caput medusa appearance)
AVM	2 (2.7)	
Venous angioma	1 (1.4)	
Cavernoma	2 (2.7)	
Normal	22 (30.1)	
Total	73 (100)	

MRI findings, and assessed the detection rate of the structural abnormalities among this group of patients on MRI.

Materials and methods

Seventy-three epileptic patients who were refractory to medical treatment were evaluated with cranial MRI within the past year. The patients were referred to our MRI unit from neurology clinics with at least one of the following criteria: intractable epileptic seizures with adequate trials of drugs within 2 years; or high frequency of epileptic seizures enough to impair the quality of life. Their ages ranged between 0 and 68 years old (mean age 15 years). Thirty-two of the patients were male, and 41 of them were female.

All of the patients were evaluated by 1.5-T MRI scanners with a standard head coil, 62 of them by 1.5-T Picker Eclipse (Picker International, Cincinnati, Ohio) and the rest of them by 1.5-T Siemens Magnetom Vision (Siemens, Erlangen, Germany). The parameters used for the patients were as follows: spin-echo (SE) T1 (TR = 439 ms, TE = 12.5 ms, flip angle = 90°), fast spin-echo (FSE) proton-density (PD) T2 (TR = 3049 ms, TE = 32, 112 ms, FA = 90°) sequences on the axial plane, FSE T2 (TR = 5289 ms, TE = 90 ms, flip angle = 90), fluid-attenuated inversion recovery (FLAIR; TR = 6000 ms, TE = 100 ms, TI = 1800 ms, flip angle = 90) sequences in the coronal plane, and SE T1 (TR = 329 ms, TE = 12.5 ms, flip angle = 90) sequence in the sagittal plane for Picker Eclipse, and the same sequences and planes with slightly changing TR/TE times for Magnetom Vision scanner. Slice thickness and interval values were 5 mm/1 mm. But additionally 3 mm of slice thickness with 0.5-mm-interval parameters were used for medial temporal lobe in the coronal plane. Spoiled 3D gradient-echo sequence with TR = 17.2 ms, TE = 6.6 ms, and flip angle = 20 with a coronal section at 1-mm partition thickness was additionally used for some patients with developmental anomalies (cortical dysplasia, heterotopia, schizencephaly cases). Spin-echo T1 sequences in three planes with intravenous gadolinium administration were obtained in the patients with herpes encephalitis, Rasmussen's encephalitis, tumoral mass lesions, tuberous sclerosis, and vascular malformations.

The assessment of MRI studies was performed by two experienced neuroradiologists in our radiology department.

Results

The pathologies in 73 patients determined by MR imaging are listed in Table 1. Cerebral infarct regions were detected in 8 of 73 patients (10.9%). Four of the patients had a history of head trauma (age range 4–56 years), two had a history of perinatal asphyxia (age range 7–9 years), and two had a cerebrovascular

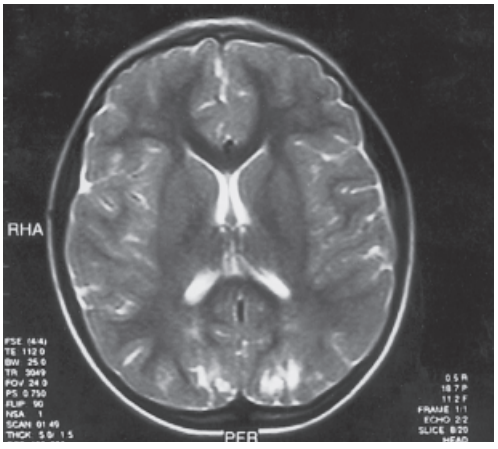

Fig. 1 T2-weighted axial MR image of a 7-year-old female patient with epileptic seizures resistant to medical therapy shows bilateral occipitoparietal encephalomalacia, involving cortical gray matter and subcortical white matter

attack (age range 47–59 years). Encephalomalacic areas were detected in the parietal–occipital lobes in 3 patients, in the frontal lobes in 4 patients, and in multiple sites in 1 patient. Magnetic resonance imaging of this subtype of patients revealed hypointense areas on T1-weighted and hyperintense areas on T2-weighted sequences, representing encephalomalacic areas associated with neighboring sulcal and ventricular enlargement (Fig. 1).

Herpes encephalitis in 2 patients (2.7%; Fig. 2) and Rasmussen's encephalitis in 1 patient (1.4%; Fig. 3) were the underlying pathologies which caused epileptic seizures. One of the patients with herpes encephalitis had a unilateral disease, whereas the other patient had a bilateral disease. The temporal, frontal, and insular areas were the involved regions. Rasmussen's encephalitis was the diagnosis in a patient with progressive frontotemporal atrophy on consecutive MRI scans and with the clinical findings of progressive left-sided hemiplegia, epilepsia partialis continua.

Cerebral tumoral mass lesions were detected in 5 patients (6.8%). One of the lesions was a well-circumscribed frontal lobe tumor located at corticosubcortical area without contrast enhancement, and causing somewhat remodeling of inner tabula of the frontal lobe, the biopsy result was dysembryoplastic neuroepithelial tumor (DNET; 1.4%). Two patients had well-circumscribed mass lesions of frontal and medial temporal lobes, the frontal mass had a mild contrast enhancement and the medial temporal mass enhanced peripherally following contrast administration. They underwent surgical resection and had the diagnosis of glial tumor (one was grade-II astrocytoma of frontal lobe, and the other was ganglioglioma of medial temporal lobe; 2.7%; Fig. 4). Two other patients had a clinical history of malignancy (lung carcinoma and breast carcinoma), and multiple mass lesions were detected on MRI scans leading to the diagnosis of metastases (2.7%).

Mesial temporal sclerosis (MTS) or hippocampal sclerosis was detected in MRI scans of 16 patients (21.9%). Mesial temporal sclerosis was the most common abnormality among the MRI-proven pathological patients (31.4%). The patients were assessed for the presence of the high signal intensity in the hippocampus on FSE T2 and FLAIR sequences, reduced hippocampal size, ipsilateral atrophy of the hippocampal collateral white matter, enlarged temporal horn, and reduced gray-white matter demarcation in the temporal lobe by visual inspection. Fourteen patients had unilateral MTS and 2 patients had bilateral MTS according to the above criteria. Reduced hippocampal size with ipsilateral atrophy of the hippocampal collateral white matter and enlarged temporal horn were detected in 14 of 16 patients (87.5%), whereas 2 patients were normal according to these parameters (12.5%). High signal intensity of the hippocampal gyrus on FLAIR sequence was the

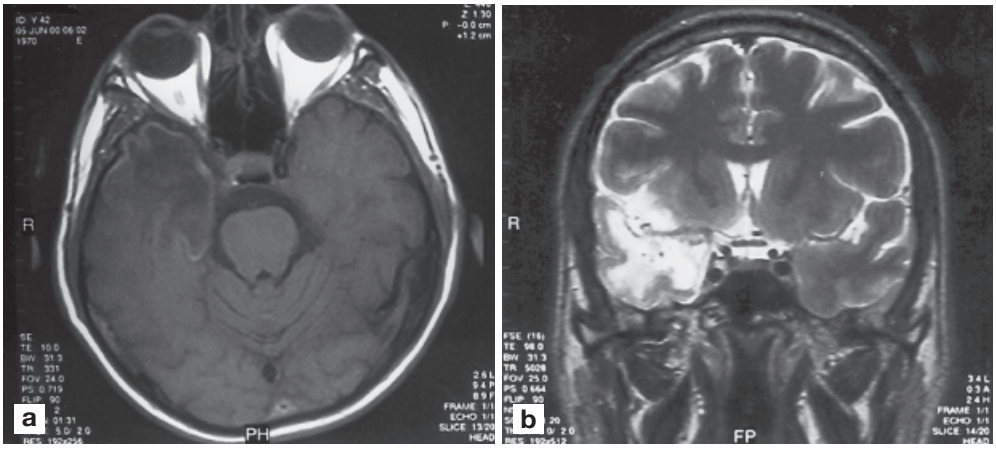

Fig. 2 **a** T1-weighted axial, and **b** T2-weighted coronal MR images of a 42-year-old male patient with intractable epileptic seizures and altered consciousness show involvement of the right temporal lobe with herpes simplex encephalitis. T1-weighted image reveals hypointense (associated gyral hyperintensity refers to the hemorrhagic nature of the disease) and T2-weighted image reveals hyperintense signal changes of the cortical gray matter and subcortical white matter

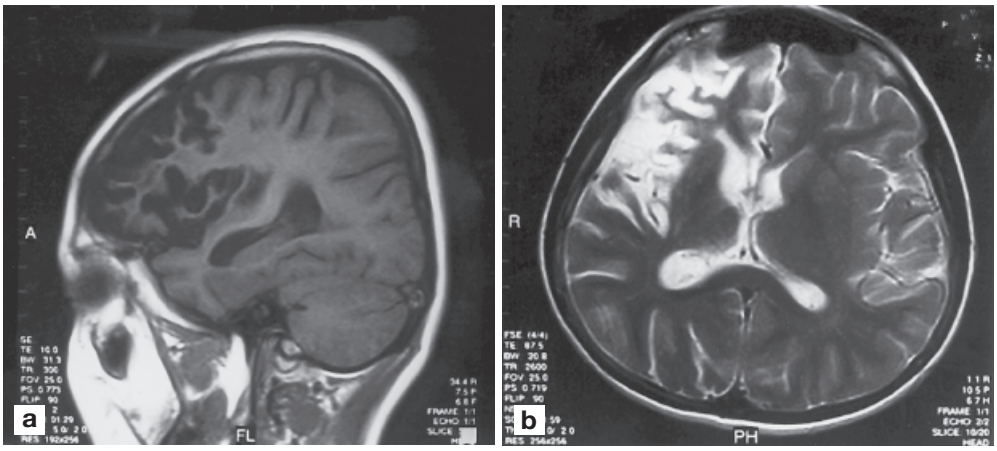

Fig. 3 **a** T1-weighted sagittal, and **b** T2-weighted axial MR images of a 12-year-old male patient with intractable epileptic seizures due to Rasmussen's encephalitis show involvement of the cortical gray matter and subcortical white matter of the right frontal and temporal lobes, dilatation of the neighboring cerebrospinal fluid spaces at the subarachnoid and lateral ventricular compartments secondary to the loss of parenchyma, and the atrophy of ipsilateral basal ganglia, thalamus, and internal capsule

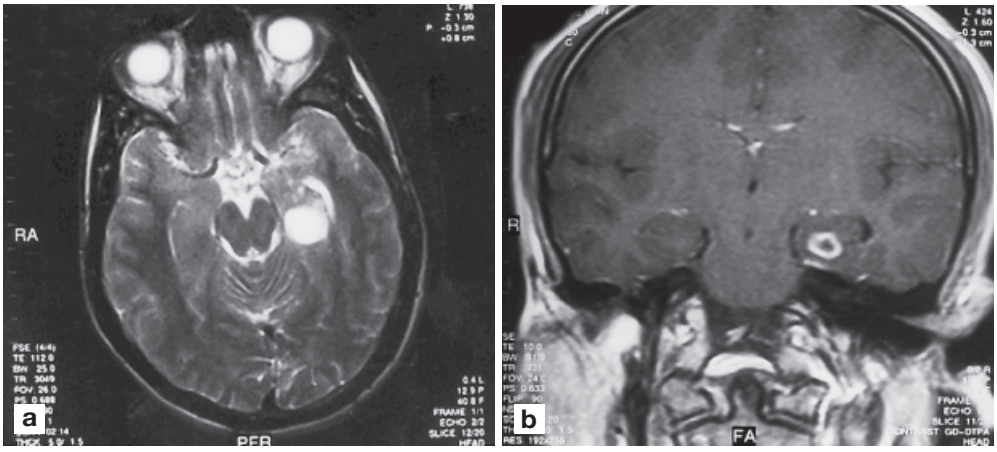

Fig. 4 **a** T2-weighted axial, and **b** post-gadolinium T1-weighted coronal MR images of a 14-year-old male patient with intractable partial-complex epileptic seizures reveal a well-circumscribed left medial temporal mass lesion, hyperintense on T2-weighted images and with peripheral contrast enhancement. Histopathological examination of the lesion led to diagnosis of ganglioglioma

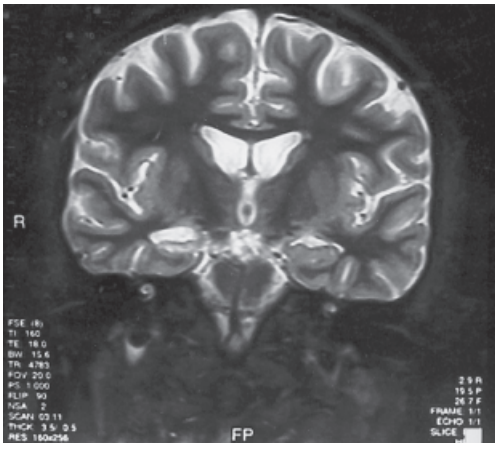

Fig. 5 T2-weighted coronal MR image of a 21-year-old male patient with intractable partial-complex epileptic seizures reveals atrophic right hippocampal gyrus with increased cortical signal intensity at that region, concordant with mesial temporal sclerosis

common finding in all of the patients with MRI-proven MTS; however, FSE T2 sequence missed one of the patients with normal size of hippocampus (Fig. 5).

Fourteen patients were detected to have a neuronal organization-migration anomaly on MRI scans (19.2 %), distributed as radial microbrain or microlissencephaly group 2 in 1 patient (1.4 %; Fig. 6), agyria-pachygyria in 2 patients (2.7 %; Fig. 7), subcortical heterotopia in 2 patients (2.7 %; Fig. 8), focal cortical dysplasia or polymicrogyria in 3 patients (4.1 %; Fig. 9), schizencephaly in 3 patients (4.1 %; Fig. 10), cerebral hemiatrophy (Dyke-Davidoff-Masson syndrome) in 2 patients (2.7 %; Fig. 11), and tuberous sclerosis in 1 patient (1.4 %).

The MRI diagnosis of microbrain (microlissencephaly type 2) was put by seeing normal thickness of cortical mantle with simplified gyral pattern and retarded myelination. Two patients had agyria-pachygyria in MRI studies; one was almost totally agyric, whereas the other had frontoparietal preservation. The cortical mantle was thick with decreased number of gyri and depth of sulci in involved areas in both of the patients.

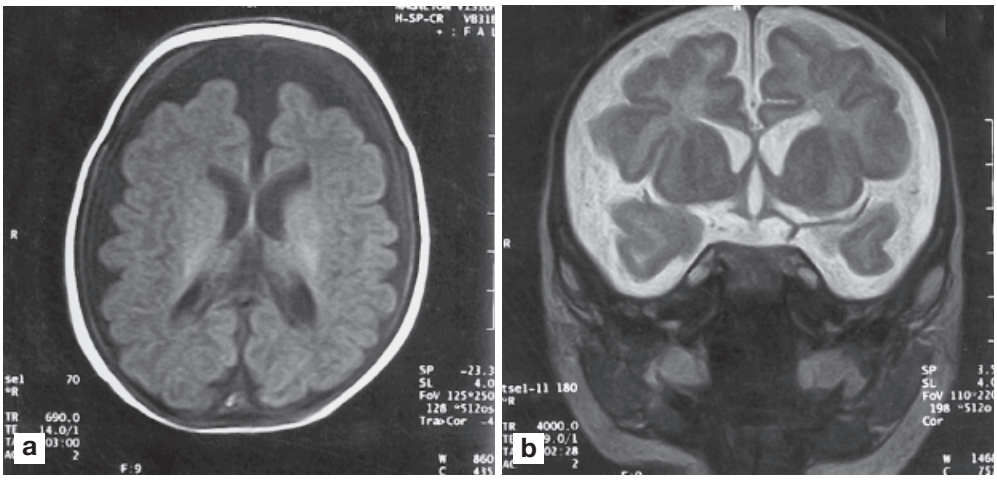

Fig. 6 **a** T1-weighted axial, and **b** T2-weighted coronal MR images of a 1-month-old male patient with medically intractable grand mal epilepsy show radial microbrain

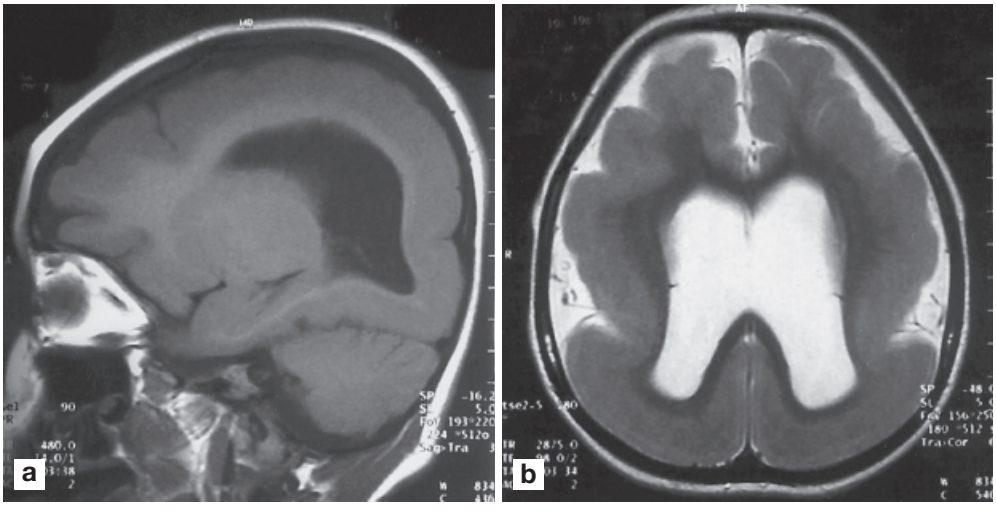

Fig. 7 **a** T1-weighted sagittal, and **b** T2-weighted axial MR images of a 9-year-old female patient with grand mal epilepsy show pachygria, involving almost whole brain

Two patients had linear bands of subcortical gray matter heterotopia of frontal lobes causing ventricular compression. The MRI pictures of three patients revealed polymicrogyria, two of them in frontoparietal regions, and one of them in bilateral perisylvian regions, characterized by multiple small and dysplastic gyral formations associated with aberrant vein in the neighboring subarachnoid space. Schizencephalic clefts lined by dysplastic gray matter were detected extending from subependymal layer to cortical layer in 3 patients; one was of parietotemporal closed-lip type, and the other two were of open-lip type in frontal and frontoparietal areas. Magnetic resonance pictures of two cerebral hemiatrophy patients showed hemiatrophy of left cerebral hemispheres and the patient with tuberous sclerosis had multiple subependymal hamartomatous nodules and cortical tubers in MRI studies.

Cerebrovascular malformations were detected in 5 patients (6.8%), 2 of which (2.7%) were arteriovenous malformations (AVM) supplied mainly from anterior circulation, 1 of which (1.4%) was developmental venous anomaly (DVA) of the parietotemporal area, and 2 of which (2.7%) were cavernous angiomas, one with frontal opercular location and one with frontal precentral gyral location (Fig. 12).

Structural MRI pathologies were detected totally in 51 patients (69.9%) in our series, whereas no MRI pathology was detected for the rest of the cases (30.1%).

Discussion

Magnetic resonance imaging is the most important neuroradiological diagnostic tool to evaluate the medically intractable epilepsy syndromes because it shows precise anatomical details of the brain with a high resolution. Recent advances in MRI have greatly enhanced our ability to visualize parenchymal anatomy. With the

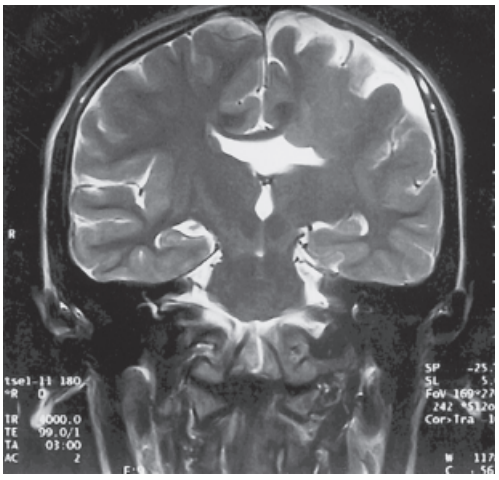

Fig. 8 T2-weighted coronal MR image of a 13-year-old female patient with secondarily generalized epilepsy shows left opercular subcortical heterotopic gray matter band causing ventricular indentation, and disruption of the overlying gyral pattern

linkage between intracranial pathology and epilepsy now clearly established, the MRI data provide detailed information for the clinician treating patients with epilepsy. A systematic approach needs to be used to review MRI scans in epilepsy patients to avoid the common pitfalls engendered by the subtle nature of many epileptogenic lesions. The hippocampus should always be evaluated especially in FLAIR sequence regardless of other MR findings to avoid missing dual abnormalities. Since epilepsy is generally a cortical process, one must search for subtle cortical abnormalities, including focal cortical infarct areas, atrophic changes, encephalitic diseases, and lesions without mass effect. Abnormal appearances of the brain should be carefully evaluated for the diagnosis of developmental abnormalities. Gray matter areas located between the cortical mantle and ventricular surface, except deep gray matter nuclei, can be indicative of gray matter heterotopia and schizencephaly. Sulcal and cortical morphological abnormalities, such as cortical thickening and small gyral formations due to lissencephalies, and cortical dysplasias, can be particularly difficult to diagnose unless a high index of suspicion is maintained. Cerebral hemiatrophy and tuberous sclerosis are easy to diagnose due to their characteristic appearances. Vascular malformations can be detected without any difficulty on MRI; however, developmental venous anomalies and the other occult vascular malformations can be easily missed [4, 6, 14, 15, 16, 17, 18, 19]. Epileptogenic foci associated with medically intractable epilepsy syndromes can be assessed on MRI with high detection rates. Structural abnormalities were detected by MRI in 82.7% of the medically intractable patients in a series of 178 patients of Zentner et al. [19].

Cerebral infarct areas associated with intractable epilepsy are primarily due to perinatal anoxia in the first years of the life, whereas vascular degeneration is primarily responsible in the late years of life. An area of encephalomalacia with a sclerotic rim around was a common MRI appearance in the cerebral infarct patients due to sclerosis, tissue loss, and astroglial proliferation developing secondary to the cerebral infarct [14, 15, 20]. Marin-Padilla [21, 22, 23] studied the neuropathology and developmental impact of perinatal brain damage in children. According to Marin-Padilla [21, 22, 23] the undamaged cortex adjacent to the injured site survives, retains its intrinsic vasculature, and is capable continuing differentiation. The postinjury alterations are not static, but ongoing processes that continue to affect the structural and functional differentiation of the still developing cortex and may eventually influence the neurological and cognitive maturation of the affected children. Marin-Padilla [21, 22, 23] proposes that the progressive postinjury reorganization of the undamaged cortex and its consequences (acquired cortical dysplasia), rather than the original lesion, represent the main

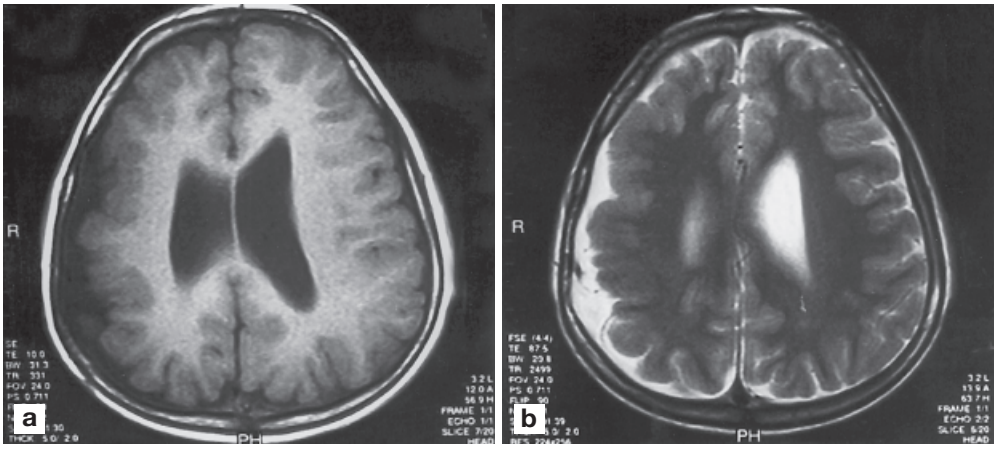

Fig. 9 **a** T1-weighted axial, and **b** T2-weighted axial MR images of a 14-year-old male patient show a wide area of polymicrogria at the right frontoparietal region, associated with widened neighboring cerebrospinal fluid spaces and with neighboring aberrant drainage vein

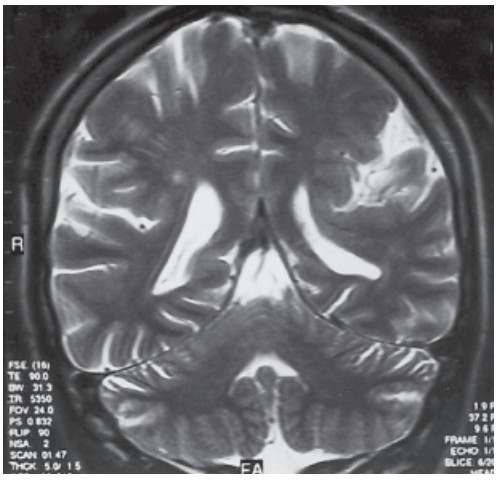

Fig. 10 T2-weighted coronal MR image of a 24-year-old male patient with secondarily generalized intractable epilepsy shows left parietotemporal closed-lip schizencephaly, extending until the left atrium, and the cortical gray matter outlining the lip is dysplastic

underlying mechanism in the pathogenesis of ensuing neurological sequelae such as epilepsy. According to Bronen et al. [15] the precise mechanism of seizures in patients who have sclerosis secondary to cerebral infarcts is unknown; however, seizures associated with cerebral infarcts secondary to perinatal and neonatal vascular insults presumably originate from gliotic tissue at the periphery of infarct areas [14].

Herpes encephalitis is a fulminant necrotic type of meningoencephalitis that usually presents with the initial involvement of temporal lobes. Typically parenchymal tissue is necrotic and hemorrhagic in appearance as in our case. Both increased T1 and T2 values on MRI are characteristic in medial temporal lobe, insular cortex, orbital surface of frontal lobe, and cingulate gyrus, mostly unilaterally, but sometimes bilaterally. The involved region becomes atrophic and gliosis develops in time [14, 15, 24, 25, 26, 27].

Rasmussen's encephalitis is a chronic localized encephalitis that is characterized by progressive hemiplegia, psychomotor deterioration, and epilepsia parsialis continua. Cortical gray matter and subcortical white matter are involved as in the case of herpes encephalitis, and it has an affinity for frontotemporal regions; involved regions atrophy in time as in the case of our patient. Because certain microscopic changes in this condition are similar to those identified in viral infections (perivascular cuffing, glial nodules, microglial proliferation), for several years Rasmussen's encephalitis was thought to be a type of viral encephalitis [14, 15, 25, 28].

In neuro-oncological series patients often have neurological deficits as the most important manifestations, symptoms of recent onset and short duration, and seizures are of secondary importance. Most histological types of brain tumors that are common in epilepsy series are rare in neuro-oncologic series [14, 15]. The most frequent tumors associated with intractable epilepsy are, in decreasing order in a study by Zentner et al. [19], gangliogliomas, pilocytic astrocytomas, and DNETs, and 98 % of the detected tumors are of low histopathological grade (World Health Organization grades I and II) [19]. The glial tumors in neuro-oncologic series are often high-grade lesions which are poorly demarcated from surrounding normal brain tissue, are associated with a peritumoral edema consistently noted, have central necrosis, and are large in size; however, tumors associated with intractable epilepsy are usually small, are well circumscribed, have minimal associated peritumoral edema, commonly cause remodeling of the inner table of the calvaria when in a cortical site, variably show enhancement, are located in the cortex rather than white matter, typically have no central necrosis, and are located supratentorially with a predilection for frontotemporal regions. The biological behavior of these tu-

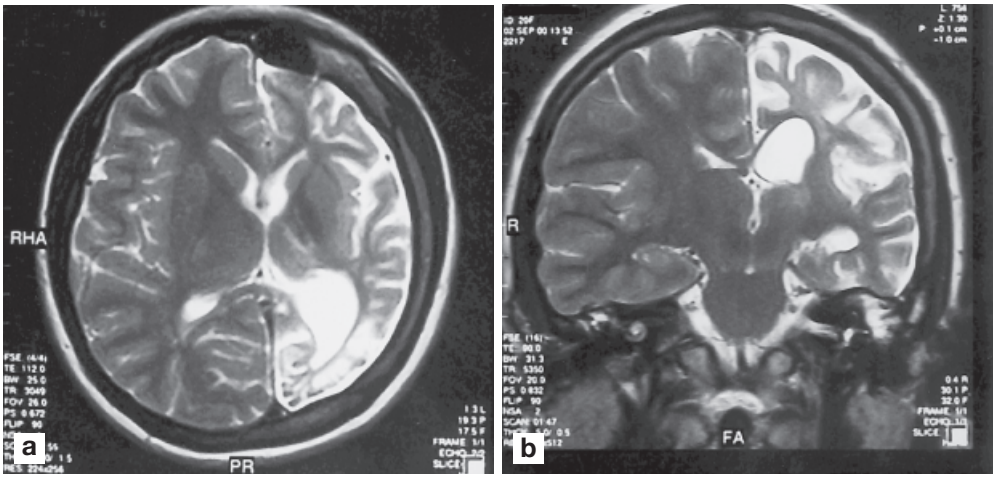

Fig. 11 **a** T2-weighted axial, and **b** T2-weighted coronal MR images of 20-year-old female patient show left cerebral hemiatrophy associated with thickened left calvarium and hyperaeration of left-sided paranasal sinuses. Ipsilateral internal capsule, thalamus, and cerebral peduncle are also atrophic. Diagnosis is Dyke-Davidoff-Masson syndrome

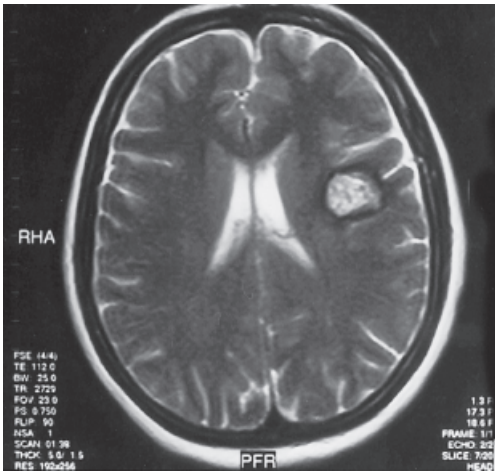

Fig. 12 T2-weighted axial MR image of a 43-year-old male patient shows left frontal opercular cavernoma

mors is strikingly indolent, as indicated by a long history of chronic seizures. They typically arise in young hosts [4, 7, 26, 29, 30]. A multicystic appearance on MRI studies is a characteristic feature of DNET and corresponds to its myxoid matrix and multinodular architecture. This feature is rare in gangliogliomas and glioneuronal malformations, and may help differentiate DNETs from these disorders [31]. Elster and Mirza evaluated 150 patients with partial epilepsy syndromes on MRI, and 69 of them were found to have associated structural abnormalities (46%); 19 patients of these 69 patients had MRI-proven tumoral mass lesions (12.7%) [32]. Another study performed by Kuzniecky et al. included 44 pediatric-age patients with partial epilepsy and MRI revealed histopathologically proven tumoral mass lesions as the underlying cause in 10 of the patients (22.7%) [33]. It is obvious that tumoral mass lesions represent an important part of the epileptogenic lesions in all age groups. The rate was 6.8% for our series, which seems to be a much lower rate compared with the previous series). The sensitivity of MRI for tumoral mass lesions is very high, and signal abnormalities on MRI were detected in 98.7% of patients with surgically proven tumors in a series of Zentner et al. [19].

Mesial temporal sclerosis is the most frequent cause of medically intractable epilepsy syndromes. In MTS, cell loss and astrogliosis occur in the mesial temporal cortex, hippocampal formation, parahippocampal gyrus, amygdala, and entorhinal cortex. As noted in autopsy studies, bilateral involvement is common and reported to be approximately 80% [9, 15, 34, 35]. The MRI counterparts of cell loss and astrogliosis are atrophy and signal change. Reports have best described these changes in the hippocampal formation. Hippocampal atrophy is best detected on coronal T1-weighted inversion recovery sequences, and the atrophy in MRI scans corresponds to cell loss. The MRI signal intensity increase on FSE T2 and FLAIR sequences are consistent with increased tissue water content [15, 17, 35, 36]. Loss of normal internal architecture in the involved hippocampus and unilateral atrophy of the mamillary body, the columns of fornix, the amygdala, and the white matter bundle in the parahippocampal gyrus are the histopathological findings detected in MTS. The reliable MRI findings of MTS can be listed as reduced hippocampal size with increased signal intensity on FLAIR or FSE T2 images, the atrophy of the hippocampal collateral white matter, enlarged temporal horn, reduced gray-white matter demarcation in the temporal lobe, and decreased temporal lobe size. But the increased hippocampal signal intensity is the most consistent finding as a study of Meiners et al. [4] implies with the histopathological correlation of MTS [37, 38, 39]; however, some patients may have a normal-sized hippocampus with an increased signal intensity on FLAIR or FSE T2 images, and some others may have hippocampal atrophy without an obvious signal change. Unilateral dilatation of the temporal horn by itself is not a reliable finding because it occurs as a common normal variant as well [4, 14, 15,19, 30, 36, 37, 38, 39]. Visual inspection and volumetric analysis of MR images allow MTS to be reliably identified in patients with temporal lobe epilepsy [35, 39, 40]. There is evidence to suggest that widespread temporal lobe pathology, leading to atrophy, may be associated with MTS, and such abnormal tissue may play an important role in epileptogenesis. The degree of atrophy in the extrahippocampal structures correlated with the degree of hippocampal atrophy, suggesting that a common process may be responsible [35, 40]. Signal abnormalities on MRI were detected in 69.2% of patients with surgically proven MTS in a series of Zentner et al. [19]. In a study of 30 patients with medically intractable temporal lobe epilepsy, performed by Meiners et al., coronal FLAIR images provide a similar or increased yield in the detection of MTS compared with T2-weighted FSE images [38, 39].

The brain is small with simplified gyral pattern and undermyelination in radial microbrain which is also classified as a subtype of lissencephaly, microlissencephaly type II. Agyria–pachygria or lissencephaly is characterized by the presence of broad malformed gyri. Subcortical heterotopia develops secondary to the arrest of radial migration of neurons at abnormal locations during intrauterine life. Polymicrogyria or focal cortical dysplasia refers to a circumscribed area of the brain with a four-layered cortex and with numerous small abnormal gyri, the lesions range from small areas, often difficult to identify, to extensive structural abnormality. Cortical malformations due to disorganization, occurring later in intrauterine life, are represented by polymicrogyria. These lesions are often bilateral and perisylvian, but at times they are unilateral and in some

patients may be occipital or frontal. Schizencephaly or agenetic porencephaly is characterized by a cleft extending from ependymal layer of the lateral ventricle to the cortex; the cleft is lined with a dysplastic cortical gray matter mantel. Schizencephaly has open-lip and closed-lip subtypes depending on the cleft type. Cerebral hemiatrophy, thickening of the calvarium, hypertrophy of paranasal sinuses and mastoid cellules on the same side are the features observed in cerebral hemiatrophy or Dyke-Davidoff-Masson syndrome. Tuberous sclerosis is characterized by the presence of the cortical tubers, calcified subependymal hamartomas, and in some cases the development of giant cell tumor at the neighborhood of foramen of Monro. Many characteristic clinical findings are associated with all the pathologies described above, but the common point for them is the presence of prolonged history of epileptic seizures. Surgical intervention is not possible with many of these pathologies, and has a low success rate if it is possible; the treatment is mostly supportive and symptomatic [8, 12, 14, 15, 27, 41, 42, 43, 44].

Vascular malformations can be detected with a high degree of sensitivity and specificity in MRI. Arteriovenous malformations consist of the dilated feeding arteries and drainage veins, and the nidus that contains thick-walled, large-diameter vessels prompting arteriovenous shunting and decreasing arteriovenous circulation time. Hemorrhage and seizures are the most common initial manifestations in the patients with AVMs. Surgical and endovascular radiological treatment of AVMs is predicated to minimize the risk of hemorrhage, and the control of seizures is frequently a secondary consideration. Cavernous hemangioma (cavernoma), capillary telangiectasia, and developmental venous anomaly are the other vascular malformations (also called occult vascular malformations) which are easily diagnosed by MRI. Cavernomas consist of large abnormal vascular spaces, surrounded by a gliotic hemosiderin-laden rim. The central nidus has a heterogeneous reticulated signal intensity, giving the characteristic MRI appearance of popcorn. Normal neurons are interspersed between the abnormal vascular channels in capillary telangiectasia; otherwise, MRI appearances of cavernomas and capillary telangiectasias are similar to each other. The primary clinical manifestation of a symptomatic cavernoma is often a chronic epileptic seizure syndrome, when surgically resected intractable seizures generally cease. In DVAs, dilated drainage veins converge on a central large draining vein, typically along an ependymal surface. Because DVAs are rarely associated with epileptic seizures, resection is rarely performed [4, 6, 14, 15, 19, 45].

Conclusion

In conclusion, epilepsy is a common neurological disorder affecting the population, a high percentage of which have medically intractable epileptic seizures associated with structural lesions of the brain. Magnetic resonance imaging has a high success rate in detecting structural brain abnormalities, of both temporal and extratemporal locations, associated with medically intractable epilepsy syndromes. Magnetic resonance imaging plays a primary role in locating and defining anatomic epileptogenic foci in the patients with intractable epilepsy so that the type of treatment and the post-interventional prognosis can be predicted by using MRI findings.

References

1. Hauser WA, Kurland LT (1975) The epidemiology of epilepsy in Rochester, Minnesota, 1935 through 1967. Epilepsia 16: 1–66
2. Taylor DC (1993) Epilepsy as a chronic sickness: remediating its impact. In: Engle JJ (ed) Surgical treatment of the epilepsy, 2nd edn. Raven, New York, pp 11–22
3. National Institutes of Health Consensus Conference (1990) Surgery for epilepsy. J Am Med Assoc 264: 729–733
4. Meiners LC, Valk J, Jansen GH, van Veelen CW (1999) MR contribution in surgery of epilepsy. Eur Radiol 9: 493–507
5. Fried I (1995) Magnetic resonance imaging and epilepsy: neurosurgical decision making. Magn Reson Imaging 13: 1163–1170
6. Zentner J, Hufnagel A, Ostertun B, Wolf HK, Behrens E, Campos MG, Solymosi L, Elger CE, Wiestler OD, Schramm J (1996) Surgical treatment of extratemporal epilepsy: clinical, radiologic, and histopathologic findings in 60 patients. Epilepsia 37: 1072–1080
7. Zentner J, Hufnagel A, Wolf HK, Ostertun B, Behrens E, Campos MG, Elger CE, Wiestler OD, Schramm J (1997) Surgical treatment of neoplasms associated with medically intractable epilepsy. Neurosurgery 41: 378–386
8. Kim SK, Wang KC, Hwang YS, Kim KJ, Kim IO, Lee DS, Yi Y, Cho BK (2000) Pediatric intractable epilepsy: the role of presurgical evaluation and seizure outcome. Childs Nerv Syst 16: 278–285
9. Bronen RA, Fulbright RK, Spencer DD, Kim JH, Lange RC, Sutilla C (1996) Refractory epilepsy: comparison of MR imaging, CT, and histopathologic findings in 117 patients. Radiology 201: 97–105
10. Bronen RA (1992) Epilepsy: the role of MR imaging. AJR 159: 1165–1174
11. Jack CR Jr (1993) Epilepsy: surgery and imaging. Radiology 189: 635–646
12. Commission on Classification and Terminology of the International League Against Epilepsy (1989) Proposal for revised classification of epilepsies and epileptic syndromes. Epilepsia 30: 389–399

13. Commission on Classification and Terminology of the International League Against Epilepsy (1981) Proposal for revised clinical and electroencephalographic classification epileptic seizures. Epilepsia 22: 489–501
14. Jack CR Jr (1996) Magnetic resonance imaging in epilepsy. Mayo Clin Proc 71: 695–711
15. Bronen RA, Fulbright RK, Kim JH, Spencer SS, Spencer DD (1997) A systematic approach for interpreting MR images of the seizure patient. AJR 169: 241–247
16. Boon P, Calliauw L, De Reuck J, Hoksbergen I, Achten E, Thiery E, Caemaert J, De Somer A, Decoo D (1994) Clinical and neurophysiological correlations in patients with refractory partial epilepsy and intracranial structural lesions. Acta Neurochir (Wien) 128: 68–83
17. Achten E, Boon P, De Poorter J, Calliauw L, Van de Kerckhove T, De Reuck J, Kunnen M (1995) An MR protocol for presurgical evaluation of patients with complex partial seizures of temporal lobe origin. Am J Neuroradiol 16: 1201–1213
18. Risse JH, Menzel C, Grunwald F, Brechtelsbauer D, Ostertun B, Kuczaty S, Biersack HJ (1999) Early childhood MRI findings in complex partial seizures and hippocampal sclerosis. J Magn Reson Imaging 10: 93–96
19. Zentner J, Hufnagel A, Wolf HK, Ostertun B, Behrens E, Campos MG, Solymosi L, Elger CE, Wiestler OD, Schramm J (1995) Surgical treatment of temporal lobe epilepsy: clinical, radiological, and histopathological findings in 178 patients. J Neurol Neurosurg Psychiatry 58: 666–673
20. Diaz-Arrastia R, Agostini MA, Frol AB, Mickey B, Fleckenstein J, Bigio E, Van Ness PC (2000) Neurophysiologic and neuroradiologic features of intractable epilepsy after traumatic brain injury in adults. Arch Neurol 57: 1611–1616
21. Marin-Padilla M (2000) Perinatal brain damage, cortical reorganization (acquired cortical dysplasias), and epilepsy. Adv Neurol 84: 153–172
22. Marin-Padilla M (1999) Developmental neuropathology and impact of perinatal brain damage. III. Gray matter lesions of the neocortex. J Neuropathol Exp Neurol 58: 407–429
23. Marin-Padilla M (1997) Developmental neuropathology and impact of perinatal brain damage. II. White matter lesions of the neocortex. J Neuropathol Exp Neurol 58: 407–429
24. Jay V, Hwang P, Hoffman HJ, Becker LE, Zielenska M (1998) Intractable seizure disorder associated with chronic herpes infection. HSV1 detection in tissue by the polymerase chain reaction. Childs Nerv Syst 14: 15–20
25. Trinka E, Dubeau F, Andermann F, Bastos A, Hui A, Li LM, Kohler S, Olivier A (2000) Clinical findings, imaging characteristics and outcome in catastrophic post-encephalitic epilepsy. Epileptic Disord 2: 153–162
26. Takahashi S, Higano S, Kurihara N, Mugikura S, Sakamoto K, Nomura H, Ikeda H (1997) Correlation of lesions in the hippocampal region noted on MR imagings with clinical features. Eur Radiol 7: 281–286
27. Zupanc ML (1997) Neuroimaging in the evaluation of children and adolescents with intractable epilepsy. I. Magnetic resonance imaging and the substrates of epilepsy. Pediatr Neurol 17: 19–26
28. Topcu M, Turanli G, Aynaci FM (1999) Rasmussen encephalitis in childhood. Childs Nerv Syst 15: 395–403
29. Aronica E, Leenstra S, van Veelen CW, van Rijen PC, Hulsebos TJ, Tersmette AC, Yankaya B, Troost D (2001) Glioneuronal tumors and medically intractable epilepsy: a clinical study with long-term follow-up of seizure outcome after surgery. Epilepsy Res 43: 179–191
30. Lee DH, Gao FQ, Rogers JM, Gulka I, Mackenzie IRA, Parrent AG, Kubu CS, Munoz DG, McLachlan RS, Blume WT, Girvin JP (1998) MR in temporal lobe epilepsy: analysis with pathologic confirmation. Am J Neuroradiol 19: 19–27
31. Ostertun B, Wolf HK, Campos MG, Matus C, Solymosi L, Elger CE, Schramm J, Schild HH (1996) Dysembryoplastic neuroepithelial tumors: MR and CT evaluation. Am J Neuroradiol 17: 419–430
32. Elster AD, Mirza W (1991) MR imaging in chronic partial epilepsy: role of contrast enhancement. Am J Neuroradiol 12: 165–170
33. Kuzniecky R, Murro A, King D, Morawetz R, Smith J, Powers R, Yaghmai F, Faught E, Gallagher B, Snead OC (1993) Magnetic resonance imaging in childhood intractable partial epilepsies: pathologic correlations. Neurology 43: 681–687
34. Lehericy S, Dormont D, Semah F, Granat O, Baulac M, Marsault C (1996) Magnetic resonance imaging of temporal lobe epilepsy. J Radiol 77: 1095–1104
35. Bronen RA, Fulbright RK, King D, Kim JH, Spencer SS, Spencer DD, Lange RC (1997) Qualitative MR imaging of refractory temporal lobe epilepsy requiring surgery: correlation witn pathology and seizure outcome after surgery. AJR 169: 875–882
36. Paterson A, Winder J, Bell KE, McKinstry CS (1998) An evaluation of how MRI is used as a pre-operative screening investigation in patients with temporal lobe epilepsy. Clin Radiol 53: 353–356
37. Meiners LC, van der Grond J, van Rijen PC, Springorum R, de Kort GA, Jansen GH (2000) Proton magnetic resonance spectroscopy of temporal lobe white matter in patients with histologically proven hippocampal sclerosis. J Magn Reson Imaging 11: 25–31
38. Meiners LC, van Gils AD, Jahsen GH, de Kort G, Witkamp TD, Ramos LM, Valk J, Debets RM, van Huffelen AC, van Veelen CW (1994) Temporal lobe epilepsy: the various MR appearances of histologically proven mesial temporal sclerosis. Am J Neuroradiol 15: 1547–1555
39. Meiners LC, van Gils AD, De Kort G, Van Der Graaf Y, Jansen GH, Van Veelen CW (1999) Fast fluid-attenuated inversion recovery (FLAIR) compared with T2-weighted spin-echo in the magnetic resonance diagnosis of mesial temporal sclerosis. Invest Radiol 34: 134–142
40. Moran NF, Lemieux L, Kitchen ND, Fish DR, Shorvon SD (2001) Extrahippocampal temporal lobe atrophy in temporal lobe epilepsy and mesial temporal sclerosis. Brain 124: 167–175
41. Edwards JC, Wyllie E, Ruggeri PM, Bingaman W, Luders H, Kotagal P, Dinner DS, Morris HH, Prayson RA, Comair YG (2000) Seizure outcome after surgery for epilepsy due to malformation of cortical development. Neurology 55: 1110–1114
42. Wyllie E (1999) Catastrophic epilepsy in infants and children: identification of surgical candidates. Epileptic Disord 1: 261–264
43. Andermann F (2000) Cortical dysplasias and epilepsy: a review of the architectonic, clinical and seizure patterns. Adv Neurol 84: 479–496
44. Hong SC, Kang KS, Seo DW, Hong SB, Lee M, Nam DH, Lee JI, Kim JS, Shin HJ, Park K, Eoh W, Suh YL, Kim JH (2000) Surgical treatment of intractable epilepsy accompanying cortical dysplasia. J Neurosurg 93: 766–773
45. Woof HK, Wiestler OD (1993) Surgical pathology of chronic epileptic seizure disorders. Brain Pathol 3: 371–380